Article

A New Polyvinylidene Fluoride Membrane Synthesized by Integrating of Powdered Activated Carbon for Treatment of Stabilized Leachate

Salahaldin M. A. Abuabdou [1], **Zeeshan Haider Jaffari** [2], **Choon-Aun Ng** [1], **Yeek-Chia Ho** [3,*] and **Mohammed J. K. Bashir** [1,*]

[1] Department of Environmental Engineering, Engineering and Green Technology Faculty, Universiti Tunku Abdul Rahman, Kampar 31900, Malaysia; sabdou6@1utar.my (S.M.A.A.); ngca@utar.edu.my (C.-A.N.)

[2] Department of Environmental Engineering and Management, Chaoyang University of Technology, No. 168, Jifeng E. Rd, Wufeng District, Taichung 413310, Taiwan; engr.zeeshanhaiderjaffari@gmail.com

[3] Centre of Urban Resource Sustainability, Department of Civil and Environmental Engineering, Institute of Self-Sustainable Building, Universiti Teknologi PETRONAS, Seri Iskandar 32610, Malaysia

* Correspondence: yeekchia.ho@utp.edu.my (Y.-C.H.); jkbashir@utar.edu.my (M.J.K.B.); Tel.: +60-5-4688888 (ext. 4559) (M.J.K.B.); Fax: +60-5-466-7449 (M.J.K.B.)

Abstract: Stabilized landfill leachate contains a wide variety of highly concentrated non-biodegradable organics, which are extremely toxic to the environment. Though numerous techniques have been developed for leachate treatment, advanced membrane filtration is one of the most environmentally friendly methods to purify wastewater effectively. In the current study, a novel polymeric membrane was produced by integrating powdered activated carbon (PAC) on polyvinylidene fluoride (PVDF) to synthesize a thin membrane using the phase inversion method. The membrane design was optimized using response surface methodology (RSM). The fabricated membrane was effectively applied for the filtration of stabilized leachate using a cross-flow ring (CFR) test. The findings suggested that the filtration properties of fabricated membrane were effectively enhanced through the incorporation of PAC. The optimum removal efficiencies by the fabricated membrane (14.9 wt.% PVDF, 1.0 wt.% PAC) were 35.34, 48.71, and 22.00% for COD, colour and NH_3-N, respectively. Water flux and transmembrane pressure were also enhanced by the incorporated PAC and recorded 61.0 $L/m^2 \cdot h$ and 0.67 bar, respectively, under the conditions of the optimum removal efficiency. Moreover, the performance of fabricated membranes in terms of pollutant removal, pure water permeation, and different morphological characteristics were systematically analyzed. Despite the limited achievement, which might be improved by the addition of a hydrophilic additive, the study offers an efficient way to fabricate PVDF-PAC membrane and to optimize its treatability through the RSM tool.

Keywords: stabilized leachate; membrane fabrication; filtration technology; phase inversion technique; powdered activated carbon (PAC)

1. Introduction

Sanitary landfills are the widely applied technique to tackle municipal solid waste (MSW). Inappropriately, the majority of these landfills do not fulfill the normal discharged limits [1]. In developing countries such as Malaysia, more than 80% of the MSW produced was received by open duping and landfill sites [2]. This resulted in the generation of highly contaminated leachate, which is the liquid generated due to the precipitation above these solid litters and could be toxic to the surrounding environment. This leachate could contaminate the sources of fresh water if not carefully treated before discharging to the environment [3]. Stabilized leachate, which is more than ten years old, has lower BOD_5/COD ratio. Thus, it is almost impossible to treat this kind of leachate using some

biological treatment technique [4]. To date, various purification techniques such as adsorption [5], coagulation [6], advanced oxidation [7], electro-Fenton [8], and combinations of these processes [9,10] have been successfully introduced to eliminate the organic contaminates from stabilized leachate. Among these techniques, membrane filtration could be one of the most suitable purification process [11]. The membranes acted as a selective barrier to achieve the objective of separation and purification. Nonetheless, there are still some shortcomings in membrane technology such as membrane fouling upon the higher contaminant concentration [12]. Fouling could affect the separation efficiency as well as permeability of membrane, which are the vital factors in the membrane filtration [13]. Several strategies, including pre-treatment of feed [14], optimization of operating parameters [15], selection and modification of membrane [16], hydraulic flushing [17], and applied field enhancement [18], have been performed to alleviate membrane fouling and water flux rate. Under different circumstances, the workability of membrane can be improved through the membrane characteristics and performance of treatment process. Hence, investigation of membrane characterization can be separated into four groups: membrane activity (permeability, surface wettability, average pore size, and porosity); morphological characterization (surface chemistry and roughness, and external and internal membrane texture); treatment efficiency (separation performance); and antifouling evaluation (pore size decrease and cake formation) [19].

Synthetic polymers such as polypropylene (PP), polyvinylidene fluoride (PVDF), and polysulfone (PS) are commonly applied in the membrane fabrication due to their higher flux, antifouling ability, and separation efficiency [20]. Among all these synthetic polymers, PVDF polymer proved to be an ideal membrane fabrication material due its durability [21], good thermal stability and higher chemical resistance [22]. Additionally, the PVDF polymer can also help to extend the membrane life, as well as reduce the damage caused by the concentrated pollutants [23]. However, the PVDF membranes antifouling capability could be enhanced due to its hydrophobic nature [24]. Many researchers have successfully applied dry–wet phase inversion technique to boost their membrane performance [25]. For instance, Zhou et al. [26] developed an ultrafiltration PVDF membrane using nanoparticles of titanium dioxide (TiO_2) and polyvinylpyrrolidone (PVP) as blended additives to increase the fouling resistance and water permeability. The addition of PVP-TiO_2 increases the average pore size and porosity of membrane, leading to the higher flux and hydrophilicity of membrane with more than 91.4% removal performance against sulfonamide antibiotics water. Moreover, polyethylene glycol and poly(acrylic acid) were also applied in the fabrication of membrane through chemical reaction with a key focus of enhancing hydrophilicity. Their batch filtration experiments clearly exhibit an increase in critical flux and a declined fouling rate. Similarly, various reports have presented effective ways to boost the antifouling abilities of PVA-based membranes due to their hydrophilic properties [27,28].

Recently, the incorporation of activated carbon (AC) on the surface of the membrane has proven to be an effective way to boost the membrane rejection performance [29]. The utilization of AC in membrane is a relatively new technology for the elimination of organic contaminates for wastewater, which not only enhances the adsorption capacity of AC, but also improves the particle removal capabilities of membrane [30].

To date, there are quite a number of studies which clearly demonstrate that the usage of PAC can significantly improve the filterability of membranes [13]. However, evaluation of PAC addition into PVDF flat sheet membranes with different concentrations, in terms of their treatment efficiency and productivity, has not been investigated. Therefore, the current study was performed to observe the potential of incorporating PAC, for the first time, into the PVDF polymeric membrane for stabilized landfill leachate purification. Furthermore, fabricated membrane was optimized using RSM technique, and the membrane properties and morphologies were systematically characterized.

2. Materials and Methods

2.1. Collection of Leachate

Leachate sample was taken form Sahom landfill site located in Perak, Malaysia, which is an operative landfill site with a daily production of 100 tonnes of MSW in average [31]. After collection of leachate sample, it was stored in a refrigerator at 4 °C. Initial leachate characterization was performed using standardized methods of water and wastewater [32]. All measurements, including dissolved oxygen (DO), colour, chemical oxygen demand (COD), 5-day biochemical oxygen demand (BOD_5), and ammoniacal nitrogen (NH_3-N), were undertaken in triplicate.

2.2. Materials

The PVDF polymer (Kynar®740) was purchased from Afza Maju trading (Terengganu, Malaysia), and utilized after drying for 24 h at 70 °C. 1-Methyl-2-pyrrolidone (NMP, 99.5%) was purchased from Sigma–Aldrich. Methanol, (99.8%) was supplied by Chem Soln. Ultra-pure distilled water (DI) was utilized throughout the experiments. PAC was purchased from R&M Chemicals. The AC was charcoal-based, and consists of sulfide, chloride, calcium, sulphate, iron, lead, zinc, and copper. This PAC density was 1.8–2.1 kg/m^3 with pH (4–7). Particle size analysis (PSA) and field emission scanning electron microscopy (FESEM) tests were used to investigate the distribution and the size of PAC particles, respectively. All these chemical materials were of analytical grade, and used without additional treatment.

### 2.3. Experiment's Design and Optimization Process

Central Composite Design (CCD) is the design method used in response surface methodology (RSM) for the membrane fabrication's experimental design [33]. Both CCD and RSM were run by version 8 from the Design Expert. For membrane dope solution design, two factors, the polymer (PVDF) weightage and the additive (PAC) weightage, were set into the CCD. Based on preliminary experiments and the extensive literature [34,35], the total mass of fabricated membrane dope was fixed at 100 g, which represents 100% of the dope weight, thus each 1 g of the dope element is equivalent to 1% weightage. The dosage of the PVDF was set within the range of 10 g to 18 g, and the amount of PAC was set within the range of 0 g to 2 g. Regarding the CCD, the alpha value was selected to be 1.0, and thus the centre points were 14.0 and 1.0 wt.% for the polymer content and additive content, respectively. The rest of the dope weight (to complete 100 g) is the NMP solvent. The total concentration of PVDF/PAC was kept at 20% (as maximum) and 10% (as minimum), as concentration higher than 20% resulted in solutions of extremely high viscosity, and was difficult to be casted on the glass plate, while clumsy, non-thick membrane was the result of using concentration less than 10%. Five responses, which are the removing efficiencies of COD, colour, and NH_3-N, as well as maximum transmembrane pressure (max. TMP), and pure water flux, were also set into the CCD to have the full design of experiments. The influence of various parameters was optimized by RSM using a combination of statistical and numerical techniques. In the current work, nine experiments were reinforced with four replications to assess the pure error [36]. The 13 different membranes were applied in double repetition and have their effluent collected. The quadratic model for every response was investigated by analysis of variances (ANOVA) to identify the results significancy, and to find the represented quadratic model after eliminating irrelevant terms. The frontal sign of each model term signifies to either antagonistic or synergistic effect on the response when it is positive or negative, respectively [4]. In RSM, it does mention that Prob > F less than 0.050 indicates model terms are significant, and Prob > F with the values greater than 0.10 indicates model term is not significant. "Not significant", in the description of lack of fit, is regarded a decent model, as it means the experimental reading is fitting the model [37]. Additionally, a good experimentally fitted data will have a higher coefficient (R^2) value. The higher the R^2 value, the closer the experimental data towards the predicted graph model by the RSM [38,39]. Selection of the best membrane takes into consideration

the membrane purification performance. Desirability value closer to 1.0 used to be selected as the ideal design for the data.

2.4. PVDF-PAC Membrane Fabrication

2.4.1. Dope Preparation

To produce the polymeric membrane, PVDF and NMP were applied as polymer and solvent, respectively. Figure 1 presents the process used for the dope preparation. Initially, the polymeric PVDF was entirely dissolved in the NMP solvent at a temperature ranged between 60 and 70 °C using a heating mantle (Figure 1a). In order to achieve a better permeate flux of the synthesized membrane, the heating mantle temperature should always be maintained within the above stated range [21]. The dope solution containing dissolved PVDF polymer in the NMP solvent was then infused into a clean Schott bottle. After that, the required amount of PAC was inserted into the dope solution to generate the dope for hybrid membrane. Lastly, the Schott bottle containing the dope solution was placed into a sonicator bath (Cole-Parmer, Vernon Hills, IL, USA) for eight hours to confirm the homogeneous mixing of the additives without any air bubbles raised in the prepared dope [40].


(a) Polymer dope preparation   (b) Adding of PAC   (c) Membrane dope sonicator
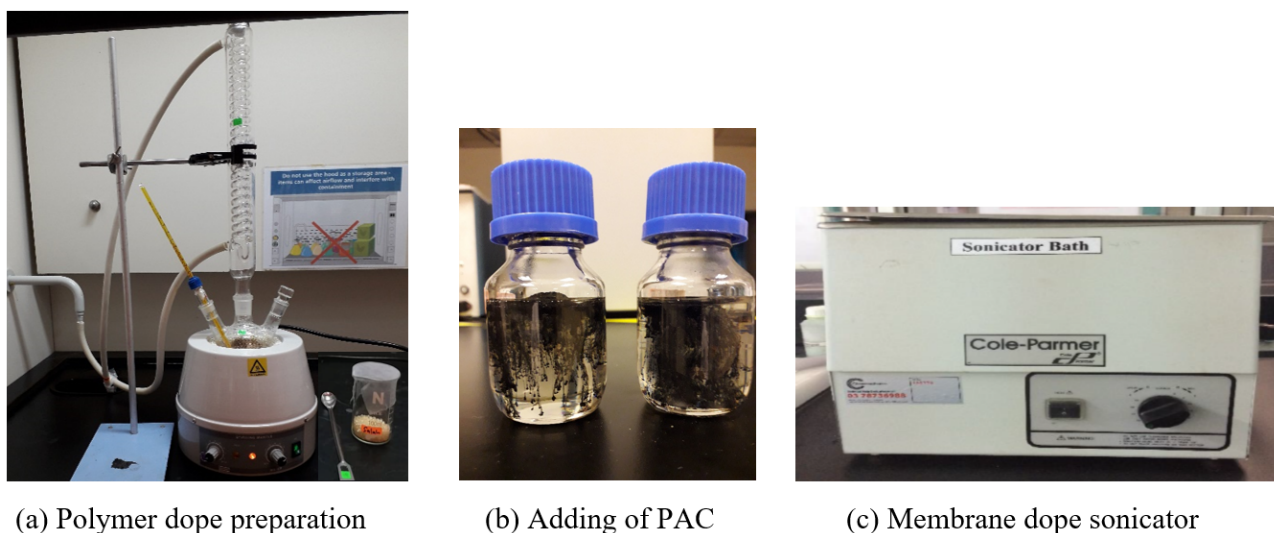
Figure 1. PVDF-PAC membrane dope preparation process.

2.4.2. Membrane Casting

A semi- automated membrane casting machine (TECH INC, Chennai, India) was applied to synthesize a flat sheet membrane using the dry–wet phase process, as illustrated in Figure 2a. The membrane was produced at temperature 27 °C to 30 °C with an approximate thickness of 60 µm based on literature reports [41,42]. After 60 s of membrane casting above the glass board, it was submerged into a distilled water (DW) basin for 180 s (Figure 2b). As a result, a thin layered polymeric film was generated, which separated from the glass plate. Later, the newly produced membrane was transferred into a DW coagulation bath and remained there for 24 h. Afterwards, a methanol bath was used for 8 h, as shown in Figure 2c, to perform a post-treatment to ensure the excess solvent in the membrane can be removed completely [43]. Finally, the membrane was dried 24 h at the ambient temperature with 60% humidity, as shown in Figure 2d, to be ready to use in the filtration process [13].

(a) Flat sheet membrane casting
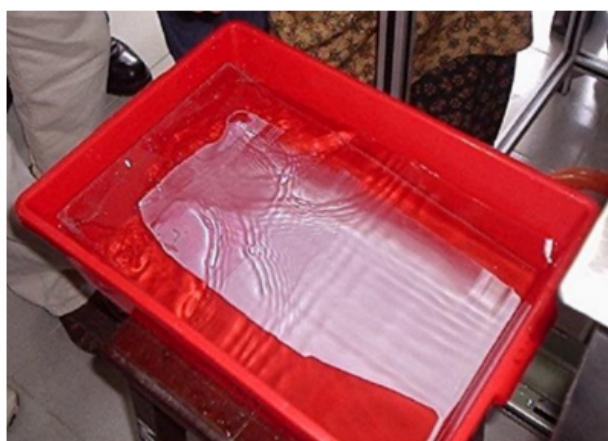
(b) Membrane solidification

(c) Membrane neutralization

(d) Membrane drying

Figure 2. The casting process of flat sheet PVDF-PAC membrane.

2.5. Membrane Performance and Characterization

The produced membranes have been characterized to investigate their treatment efficiencies, fouling, and permeability properties and surface morphologies. To ensure the accuracy of the findings, all of the tests have been duplicated. Each time, a fresh membrane has been utilized to investigate their characteristics and performance.

2.5.1. Treatment Efficiency

The membrane filtration performance was investigated using laboratory scale cross-flow filtration setup with a 3.34 cm disc diameter, as exhibited in Figure 3. The membrane rejection capabilities were studied against the treatment of landfill leachate. Before each experiment, initial characterization of leachate was measured to eliminate the small errors which occurred due to the minor changes in organics concentration with time. The steady flux for all individual membranes was acquired by a constant (200 mL/min) flow for 120 min. The volume of permeate, along with the recorded transmembrane pressure, were noted down under the flow of 200 mL/min for different intervals of time (0.5, 1, 2, 5, 10, 20, 40, 90, and 120 min).

Figure 3. CFR test configuration (filtration treatment set).

Final leachate characterizations were evaluated in terms of removing efficiencies for the COD, colour, and NH_3-N pollutants using Equation (1):

$$\text{Removal eficiency } \% = \frac{(C_F - C_P)}{(C_F)} \times 100(\%) \tag{1}$$

where C_F is the contaminant concentration at the feed (mg/L) and C_P is the contaminants concentrations in the permeated solution (mg/L). All contaminants' concentrations were checked using the UV-V spectrophotometer (Hach DR6000, Loveland, CO, USA) in prior and post of filtration practice.

2.5.2. Productivity of Membrane

Pure flux plays a dynamic role in the membrane productivity evaluation. Permeability of membrane was investigated through the pure water flux, which was measured via a dead-end filtration apparatus, as illustrated in Figure 4. A metallic ring having 5 mm average pore size and 8.76 cm^2 effective permeate area was applied to support the membrane. Initially, the impurities present in the membrane were removed by submerging the membrane in DW for 30 min. Then, a stable flux was achieved by pre-compacting the membrane with N_2 gas at a pressure of 30 KPa for 2 min. After 30 min, the permeated water volume was noted at a similar pressure of 30 KPa. The pure water flux can be calculated using the Equation (2):

$$J = \frac{V}{A \times t} \ (\text{L/m}^2 \cdot \text{h}) \tag{2}$$

where V is the permeated pure water volume (L), A is the membrane effective surface area (m^2), and t is the time of permeation (h).

Figure 4. Dead-end test (pure water permeation set-up).

2.5.3. Antifouling Valuation

Throughout the membrane filtration process, the overall decrease in flux, alongside the improvement of transmembrane pressure, were mainly caused by either membrane fouling, concentration polarization, or a combination of both [44]. Both of these components can be attained from the experimental data using both of the leachate permeate flux and maximum transmembrane pressure (Max. TMP) values which are measured by the cross-flow ring test. Max. TMP was applied to indicate the antifouling ability of fabricated membranes [45].

2.5.4. Morphological Characteristics

It is a well-known fact that the membrane properties and performance are highly dependent on its morphology (pore size, surface texture, and microstructure). Therefore, investigation of membrane morphologies is considered a significant factor in the effectiveness evaluation of the produced membranes.

Fourier transform infrared spectroscopy (FTIR, Perkin Elmer Lambda 35, Waltham, MA, USA) was applied to investigate the membrane surfaces chemical compositions. The FTIR spectra ranged between 4000–400 cm^{-1}.

EDX is a chemical microanalysis method used for quantitative, qualitative, and elemental mapping examination. Octane Silicon Drift Detector (SDD, EADX Inc., Mahwah, NJ, USA) was used at high voltage of 15 kV, using Mn Kα as source of energy. The fabricated PVDF-PAC membranes with different compositions were measured by INCA Energy 400 software (Firmware INCA, Version V1.09R13), along with the image taken by the Quanta FEG 450 instrument.

FESEM (Quanta FEG 450, FEI, Hillsboro, OR, USA) was applied to record the cross-sectional and surface morphologies of the fabricated membrane. The cross-sectional morphologies were investigated by fracturing the membranes in liquid nitrogen and immediately cutting them after air drying. FESEM measurement starts by placing the sample on carbon tape, which was attached with the sample stub. The sample was also coated with the platinum nanoparticles in auto fine coater (JFC-1600, SUTD-MIT International Design Centre, Singapore) before performing the analysis.

An atomic force microscopy (AFM, Dimension 5000, Bruker AXS, Santa Barbara, CA, USA) was also applied to study the surface morphologies and roughness of the synthesized membranes. Herein, membranes were cut into small square pieces (1 × 1 cm) and pasted on a glass slide. Sample scanning were performed using a probe-optical microscope on tapping mode and images of 10 μm × 10 μm were taken by AFM. The root-mean-square

roughness (R_q) and average roughness (R_a) was applied to measure the surface roughness for each membrane.

Porosity of membrane could be easily defined as the pore's volume divided by the membrane total volume. Wet membranes were weighed after carefully wiping the surface (Ww). Afterwards, these membranes were dried in an oven at 50 °C for 24 h and weighed again (Wd). The porosity of membrane ε (%), was measured by gravimetric method using Equation (3) [25]

$$\varepsilon = \frac{(Ww - Wd)/\rho w}{\frac{Ww - Wd}{\rho w} + Wd/\rho p} \times 100\% \tag{3}$$

where, Ww is the weight of wet membrane (kg), Wd represents the weight of dry membrane (kg), ρw is the density of water (1000 kg/m^3), and ρp, the polymer density (1770 kg/m^3 for PVDF).

Based on the measured distilled water flux, the average pore size (d) of the membrane was calculated by the Guerout–Elford–Ferry equation, Equation (4) [46].

$$d = \sqrt{\frac{(2.9 - 1.75\varepsilon)8\delta l V}{\varepsilon \, A \, \Delta P \, t}} \tag{4}$$

Herein, ε is membrane porosity (%), δ, the water viscosity (8.9×10^{-4} Pa s), l represents membrane thickness (60×10^{-6} m), V is the volume of the distilled water penetrating through the membrane (m^3), t is the experimental time interval (s), A, the effective membrane surface area (m^2), and ΔP is the working pressure (30 kPa).

3. Results and Discussion

3.1. Landfill Leachate Characteristics

Table 1 displays the key characteristics of the raw leachate sample of more than 10 years in age. The lower BOD$_5$ to COD ratio (0.074) was another strong indication of highly stabilized leachate sample [3]. The other quality parameters of leachate, such as COD, BOD$_5$, NH$_3$-N, colour, and pH values, were around 1188 mg/L, 89 mg/L, 313 mg/L, 1360 PtCo/L, and 8.33, respectively. These obtained values were also compared with the standard discharged limits set by the Malaysian Environmental Quality was conducted (Table 1) [47]. As shown in Table 1, the COD, colour, and NH$_3$-N concentrations were found to be far greater than the standard discharged limits.

**Table 1.** Raw leachate characteristics.

Parameter	Unit	Value Range	Average	Malaysia Discharge Standards
DO	mg/L	2.43–5.19	3.81	-
COD	mg/L	846–1530	1188	400
BOD$_5$	mg/L	55–122	89	20
BOD$_5$/COD	-	0.065–0.080	0.074	0.05
Colour	PtCo/L	1040–1680	1360	100
NH$_3$-N	mg/L	164–462	313	5
Suspended Solids	mg/L	75.0–80.0	77.5	50
pH	-	7.97–8.68	8.33	6.0–9.0
Turbidity	NTU	15.9–70.2	43.1	-
Electrical Conductivity	mS	13.22–22.77	18.00	-
Temperature	°C	27–30	28	40

3.2. PAC Characterization

Analysis test of the particle size was conducted to investigate the particle size distribution of fine samples in terms of volume. The particle size distribution of PAC sample is shown in Figure 5a. It can be seen from Figure 5 that PAC has small particle sizes which

varied between (0.02–50 μm) in diameter. The average particle diameter of the PAC is 25 μm. It is evident from Figure 5a that the distribution curve of PAC particles could be counted a uniform-distribution curve. The percentage of adsorption is higher for those adsorbents have smaller particle size due to the availability of more surface area [48]. The surface morphology of PAC was visualized via FESEM, with a magnification of 10,000×, as shown in Figure 5b. FESEM micrographs of PAC, shows uniform size particles, which confirmed the results obtained from the particle size analysis. To some extent, the PAC surface having small cavities, pores, and more rough surfaces indicates the presence of an interconnected porous network. Increasing the particles' number of an adsorbent material by decreasing its particles size resulted in increasing the adsorption surface area, and thus the material adsorption characteristics [49].
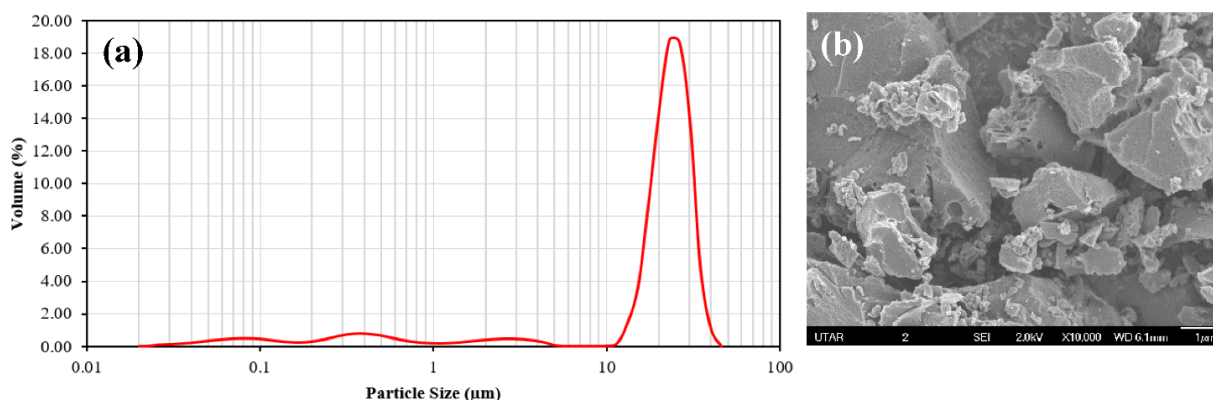
Figure 5. PAC characterization: (**a**) Particle size distribution; (**b**) FESEM image at 10,000× magnification.

3.3. Membrane Filtration and Experimental Results

Herein, the relationship among the independent factors (PVFD and PAC dosage in membrane) and responses (COD, NH_3-N, colour removal, max. TEM, and pure water flux) were thoroughly investigated. There were 13 different experiments performed on the PVDF and PAC composition based on the central RSM composite design, as shown in Table 2. CFR test was performed to investigate the pollutants removal efficiency together with the max. TEM, while dead-end test was executed to measure the pure water flux.

Table 2. Experimental results for the PVDF-PAC membranes (RSM design).

	Factors		Responses				
Run Order	**PVDF (wt.%)**	**PAC (wt.%)**	**Removal Efficiency (%) ***			**Pure Water Flux ** (L/m^2·h)**	**Max. TMP (bar)**
			COD	**Colour**	**NH$_3$-N**		
1	10.00	0.00	14.8	15.1	10.9	90.2	0.46
2	10.00	2.00	29.1	42.3	7.5	127.7	0.42
3	12.00	1.00	32.2	44.6	18.3	89.3	0.48
4	14.00	0.50	28.2	39.6	19.6	64.0	0.66
5	14.00	1.00	37.2	56.3	23.8	79.9	0.67
6	14.00	1.00	35.5	50.3	19.3	72.9	0.63
7	14.00	1.00	35.5	56.2	21.3	72.2	0.62
8	14.00	1.00	35.7	51.1	21.5	70.3	0.61
9	14.00	1.00	32.2	51.5	19.9	69.9	0.60
10	14.00	1.50	33.2	52.7	19.2	83.1	0.55
11	16.00	1.00	37.1	41.0	22.5	31.8	0.68
12	18.00	0.00	29.1	26.7	21.2	26.2	1.00
13	18.00	2.00	20.9	15.6	17.3	32.9	0.78

* Estimated by Equation (1). ** Estimated by Equation (2).

The COD, colour, and NH_3-N removal efficiencies were found to be around 14.8–37.2, 14.6–56.3, and 7.5–23.8%, respectively, while the pure flux and max. TMP were ranged between 26.2–127.7 $L/m^2 \cdot h$ and 0.42–1.00 bar, respectively. ANOVA analysis was performed for the further investigation on the obtained experimental results.

It is observed from Table 2 that an increase in both PVDF and PAC concentrations on the membrane leads, to some extent, to an increase in the contaminants removal. When PVDF and PAC concentration are higher than 14 wt.% and 1.0 wt.%, respectively, the removal efficiency starts to decrease with increasing the amount of PVDF and PAC. This behaviour was attributed to the combination effect between polymer and additive in dope. This leads to the creation of large volume voids with increasing polymer dosage, and allows the small particles of contaminants to pass through the membrane [50].

3.3.1. Removal Efficiency of Contaminants

Table 3 depicts the empirical model using the data obtained from COD, colour, and NH_3-N removals. F-values of the model, together with the low probability values (P > F > 0.05), clearly suggest that the models were significant for all responses.

Table 3. ANOVA results and quadratic models of PVDF-PAC membranes for COD, colour, and NH_3-N removal efficiencies.

Source	COD Removal (%)		Colour Removal (%)		NH_3-N Removal (%)	
	F-Value	Prob > F	F-Value	Prob > F	F-Value	Prob > F
Model	25.62	0.0002 (S) [a]	31.93	<0.0001 (S) [a]	24.34	0.0003 (S) [a]
A-PVDF (wt.%)	4.34	0.0759	3.89	0.0840	55.81	0.0001
B-PAC (wt.%)	4.19	0.0800	5.69	0.0441	6.37	0.0396
AB	32.25	0.0008	21.10	0.0018	0.032	0.8634
A^2	0.42	0.5375	97.03	<0.0001	0.24	0.6372
B^2	12.18	0.0101	-	-	3.62	0.0988
Lack of Fit	1.39	0.3665 (NS) [b]	3.27	0.1386 (NS) [b]	0.17	0.9088 (NS) [b]
	Std. Dev.	1.98	Std. Dev.	4.28	Std. Dev.	1.40
	Mean	30.85	Mean	41.69	Mean	18.64
	R^2	0.9482	R^2	0.9411	R^2	0.9456
	Adj R^2	0.9112	Adj R^2	0.9116	Adj R^2	0.9067
	C.V. %	6.42	C.V. %	10.26	C.V. %	7.52

[a] Significant. [b] Not significant.

The significant model terms for COD removals in the ANOVA analysis were sorted in descending order depending upon the influential terms (AB, B^2, A, B, and A^2). It was clearly seen that the PVDF and PAC (AB) had the highest impact on the COD removal with an F-value of around 32.25, followed by the quadratic term of PAC concentration (B^2), PVDF concentration (A), PAC concentration (B), and finally the quadratic term of PVDF concentration (A^2) with an F-value of 12.18, 4.34, 4.19, and 0.42, respectively. The quadratic terms of PVDF concentration together with the linear terms of PAC and PVDF contents caused a positive effect on the COD removal. Nonetheless, interaction and quadratic terms of PAC exhibited negative effects. In fact, an increase in the COD removal was recorded upon the change in the liner terms of PVDF and PAC concentrations, and PVDF concentration with quadratic term from lower to higher level. Hence, this change is complemented by the outstanding COD removal using PVDF-PAC membrane. On the other hand, a decline in COD removal was recorded when the interaction term and quadratic term of PAC was in the higher level.

The quadratic term of PVDF contents (A^2) has the most significant effect towards the colour removal rate. This is due to the highest F-value (97.03), where other terms had the values of 21.10, 5.69, 3.89, respectively. The PAC content (B) had a progressive influence on the colour removing. However, the quadratic term of PVDF, PVDF concentration, and interaction among the PVDF and PAC displayed a negative effect. Thus, the removal of colour was enhanced with the enhancement of the PVDF contents in membrane fabrication until the optimum amount (>14 wt.% PVDF).

Additionally, in case of NH_3-N removal, the A, B, B^2, A^2, and AB were sorted in descending order of their effecting strength. The highest F-value of 55.81 was recorded for the linear term of PVDF concentration (A), and thus it had the huge effect in NH_3-N removal. On the other hand, the lowest F-value of 0.032 was recorded for interaction term, which regarded to have a negligible effect on the model. The PVDF linear term only offered a strong influence on removing of NH_3-N, while the remaining terms were found to be the negligible influencers. Hence, the NH_3-N removal was increased upon enhancing the PVDF contents in membranes. However, for PAC concentration after the point (PAC = 1.0 wt.%); when either the quadratic term of PVDF or PAC, or the interaction term is in the significant level, the NH_3-N removal starts to decrease.

The lack of fit F-statistic was statistically not significant, as the values of (P) were higher than 0.05. A significant lack of fit suggests that there may be some systematic variation unaccounted for the proposed models. This may be due to the exact replicate values of the independent variables in the models that provide an estimate of pure error [15]. The correlation coefficient value (R^2) resulted in the present study for COD removal (0.9482), colour removal (0.9411), and NH_3–N removal (0.9456), indicating that only 5.18, 21.09, 5.89, and 5.44% of the total dissimilarity might not be explained by the empirical models. Zielinska et al. [10] stated that the correlation coefficient should be more than 0.80 for a good fit of a model. Moreover, the C.V.% of the obtained models for COD, colour, and NH_3-N removals were 6.42%, 10.26%, and 7.52%, respectively, which designates an adequate model [51].

In the current study, all insignificant model terms which have limited effects were eliminated from the study to improve the model. Based on the findings, the response surface models for COD, colour, and NH_3-N removal efficiency were constructed to predict responses, which were considered reasonable. The final regression models, in terms of their coded factors, are expressed by the second-order polynomial equations, and are presented in Table 3.

Typically, it is vital to study the effect of the operational factors on the different responses. The effect of PVDF and PAC concentration on the responses of COD, colour, and NH_3-N removals over PVDF-PAC membranes could be evaluated using perturbation and three-dimensional (3D) response surface plots (Figure 6). Perturbation plots show the comparative effects of independent variables on the responses. For instance, in Figure 6, the different sharp curvatures in PVDF concentration (A) and PAC concentration (B) show that the three responses (COD, colour, and NH_3-N removal efficiency) were very sensitive to the fabrication variables, but with different behaviours. In other words, PVDF and PAC contents have a major function in the treatment process under the experimental conditions. This is another confirmation of the important effects of the independent variables (PVDF and PAC concentrations) on the treatment removal efficiency. Therefore, the 3D surface response and contour plots of the quadratic models were utilized to assess the interactive relationships between independent variables and responses. The 3D response surface was introduced as a function of PVDF and PAC concentrations. Figure 6a,c shows a symmetrical 3D surface response for both COD and NH_3-N removals. In the meantime, the removal of colour presents a different 3D surface (Figure 6b), which indicates that colour removal was influenced differently by experimental factors than the other responses.
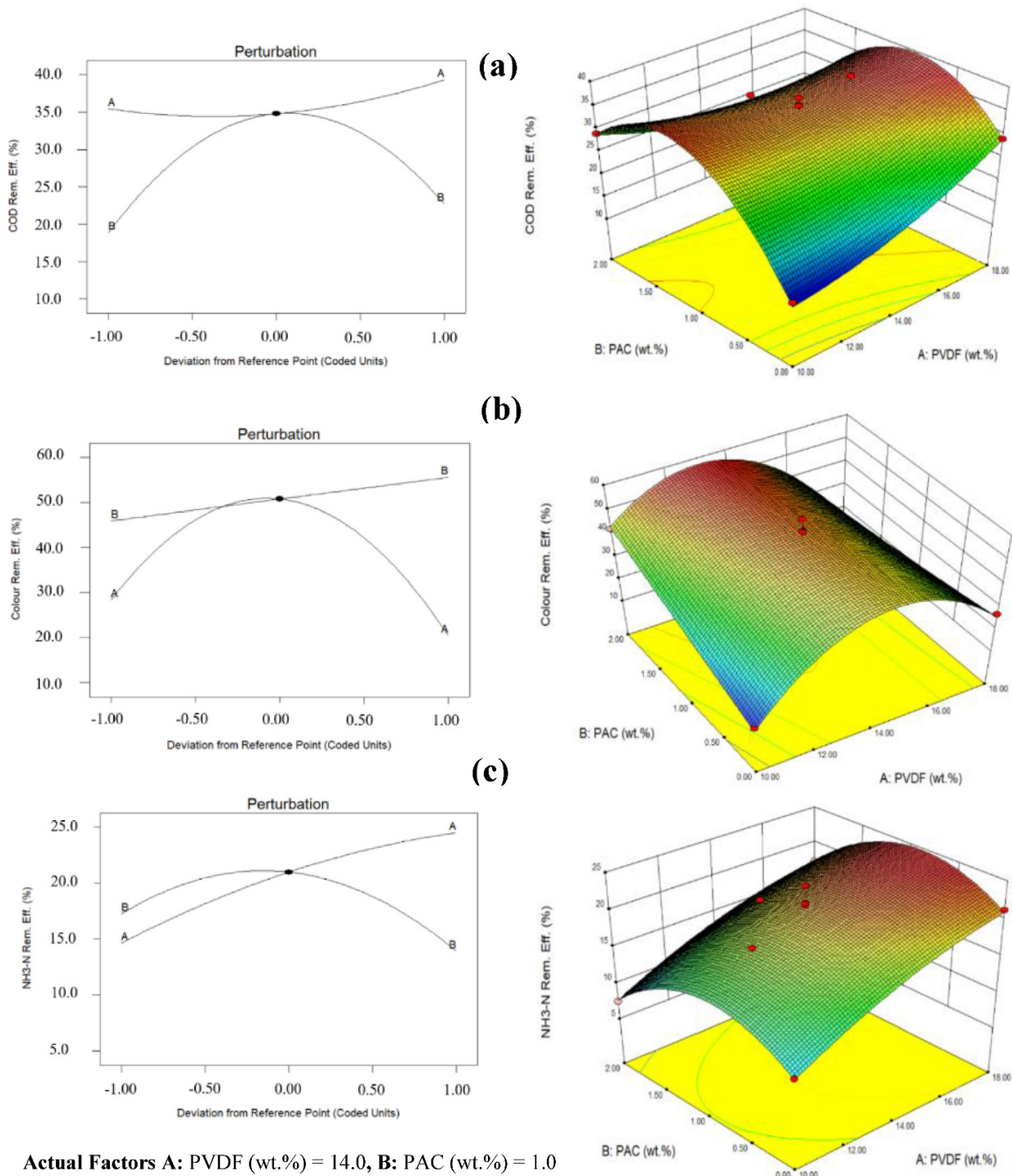
Figure 6. Perturbation plots (**left**) and 3D response surface (**right**) of PVDF-PAC fabricated membrane for the removing efficiency of (**a**) COD, (**b**) colour, and (**c**) NH$_3$-N.

Figure 6a,c indicated that the responses for COD and NH$_3$-N removal rate was sufficiently enhanced upon the increase in PVDF contents in applied membranes. On the other hand, the increase in PAC contents in membrane fabrication led, to the removal of COD and NH$_3$-N to some extent. It was seen that, when the PAC contents in membrane were higher than 1.0 wt.%, the removal rate for COD and NH$_3$-N began to decline. According to Figure 6c, for the removal of NH$_3$-N, the effect of interaction between PVDF and PAC concentrations have a noteworthy influence on removal percent. The NH$_3$-N removal were

gradually increased with the increasing of PAC concentration to some extent, which means that the incorporated PAC has enhanced the membrane performance in terms of NH_3-N removal, in addition to the main separation action gained by the membrane texture itself. This good result might be ascribed to the high adsorption characteristics of the used PAC, which significantly improved the fabricated membrane efficiency [5,52].

However, PVDF concentration has limited effect on COD removal efficiency compared with the PAC content. Where 35.5 and 38.5% of COD were removed at minimum and maximum PVDF concentration (10.0 and 18.0 wt.%), respectively, 18.5 and 35.5% of COD removal were removed at minimum and medium PAC concentration (0.0 and 1.0 wt.%), respectively. Likewise, the minimum NH_3-N removal was found to be 7.5% at membrane concentration of 10.0 wt.% PVDF and 2.0 wt.% PAC, while the maximum NH_3-N removal (24.5%) was observed at the PVDF and PAC concentration of 18.0 and 1.0 wt.%, respectively.

On the other hand, the 3D response surface in Figure 6b displays a different effect of interaction between the experimental factors on the colour removal rates. It was observed that an increase in the concentration of PVDF in the membrane leads to an improvement in the colour removal to some degree. When the concentration of PVDF was higher than (14 wt.%), the colour removal performance starts to decrease. This behaviour was credited to the combined effects of additive and polymer in the dope. This leads to creating large volume voids with increasing polymer dosage, and lets the fine particles from contaminants to permeate through the membrane [50]. Meanwhile, the enhancement of PAC concentration in a membrane drove a steady increase in the colour removal efficiency. As witnessed in Figure 6b, the predicted minimum and maximum efficiencies of colour removal were 15.0 and 56.5% present at fabrication concentrations of (18.0 wt.% PVDF, 0.0 wt.% PAC), and (14.0 wt.% PVDF, 1.0 wt.% PAC), respectively. This also confirms the effectiveness of PAC content in enhancing the removal performance of the filtration process using PVDF fabricated membrane.

Despite the incorporation of PAC into membrane enhancing the COD, colour, and NH_3-N removal, the filtered leachate still did not meet the Malaysian Discharge Standard (Table 1). This is due to the highly concentrated pollutants of leachate that resulted in a reduction in membrane efficiency owing to the clogging caused by influent SS component. Therefore, a pre-treatment process such as PAC adsorption is suggested to be used before the membrane treatment [33].

3.3.2. Pure Flux and Transmembrane Pressure Studies

By applying the factorial regression analysis on the experimental data related to PVDF-PAC membranes, both max. TMP and pure water flux responses were well agreed to a linear model of the second degree, as shown in the ANOVA analysis presented in Table 4. In a general linear model or a multiple regression model: $Y = \beta_0 + \sum_{i=1}^{k} ss_i\, X_i + \varepsilon$, where: Y is the response, X_i is the independent factor, k is the number of variables, β_0 is the constant term, β_i represents the coefficient of the linear, and ε is the random error or noise [53]. The final linear models obtained for each response has been expressed by the first order polynomial equation, as presented in the last raw of Table 4.

The fitted model for the pure water flux suggests a large F-value (53.56), suggesting that the model is significant. As the value of Prob > F of all terms is less than 0.050, this suggests that all the model terms are significant. Based on their F-values, the PVDF concentration term (A) has the highest influence on the model, followed by PAC concentration term, and lastly the combination term. The term of PAC concentration presents a positive effect on pure flux, while the other two terms have been found to be negative influencers. Hence, the pure water flux was raised only with enhancing PAC contents in the membrane while, in contrast, it is decreased with the increasing of the PVDF content of a membrane.

Table 4. ANOVA results and quadratic models of PVDF-PAC membranes for pure flux and max. TMP.

| Source	Pure Flux (L/m^2·h)		Max. TMP (bar)	
	F-Value	Prob > F	F-Value	Prob > F
Model	53.56	<0.0001 (S) [a]	49.62	<0.0001 (S) [a]
A-PVDF (wt.%)	144.45	<0.0001	131.07	<0.0001
B-PAC (wt.%)	11.86	0.0073	13.01	0.0057
AB	4.38	0.0658	4.78	0.0566
A^2	-	-	-	-
B^2	-	-	-	-
Lack of Fit	5.18	0.0681 (NS) [b]	3.38	0.1307 (NS) [b]
	Std. Dev.	7.36	Std. Dev.	0.041
	Mean	70.03	Mean	0.63
	R^2	0.9470	R^2	0.9430
	Adj R^2	0.9293	Adj R^2	0.9240
	C.V. %	10.50	C.V. %	6.56
Model equation coded, (wt.%)	+70.03 −41.68 * A +11.94 * B −7.70 * A * B		+0.63 +0.22 * A −0.070 * B −0.045 * A * B	

[a] Significant. [b] Not significant.

On the other hand, the suggested model of max. TMP was significant with a high F-value (49.62), as can be seen from Table 4. Based on its effect on the model from the highest to the lowest, the model terms can be arranged as follows: PVDF content, PAC content, and the combination of both, with F-values of 131.07, 13.01, and 4.78, respectively. However, the PVDF concentration is the only factor which showed a positive influence on the max. TMP, due to the positive sign of its term; this indicates a worse impact on the max. TMP, as it could be increased with the increasing of PVDF content on the fabricated membrane. On the other hand, PAC concentration exhibited a better effect on the max. TMP, which showed a reduction in max. TMP occurred due to the increasing of the PAC content.

Additionally, both of the models display a non-significant lack of fit F-value, which indicates that well fitted models have been selected to present the experimental results with minor pure errors [15].

The R^2 values obtained in the present study for pure flux and max. TMP were 0.9470 and 0.9430, respectively. The high value of R^2 represents good agreement between the observed and the calculated results within the experimental ranges [37]. Moreover, C.V. % for the water flux and TMP were 10.50% and 6.56%, respectively. Where these small values indicate good fitness of the models [51].

Based on these findings, the resulted response surface models in the current work for predicting the two responses (pure flux and max. TMP) were considered reasonable.

The influence of integrated PAC and the interaction of content's concentrations on the max. TMP can be explored by the plots of perturbation and 3D response surface, as shown in Figure 7. From perturbation plots at Figure 7, it is easy to notice that pure flux and max. TMP responses are very sensitive to the experimental factors, and to conclude that both have a different (inversed) behaviour regarding the PVDF and PAC concentration values. As can be seen from Figure 7a, increasing of PVDF concentration (A) resulted in a linear decrease in pure water flux and increase in max. TMP, which attributed to the reduction in membrane porosity due to the increase in polymer concentration, which is well recognized for the system of a single polymer casting solution [50]. However, PAC concentration (B) showed a different effect, as any increase in its value causes a linear increment on the pure water flux, but a decrease in max. TMP.
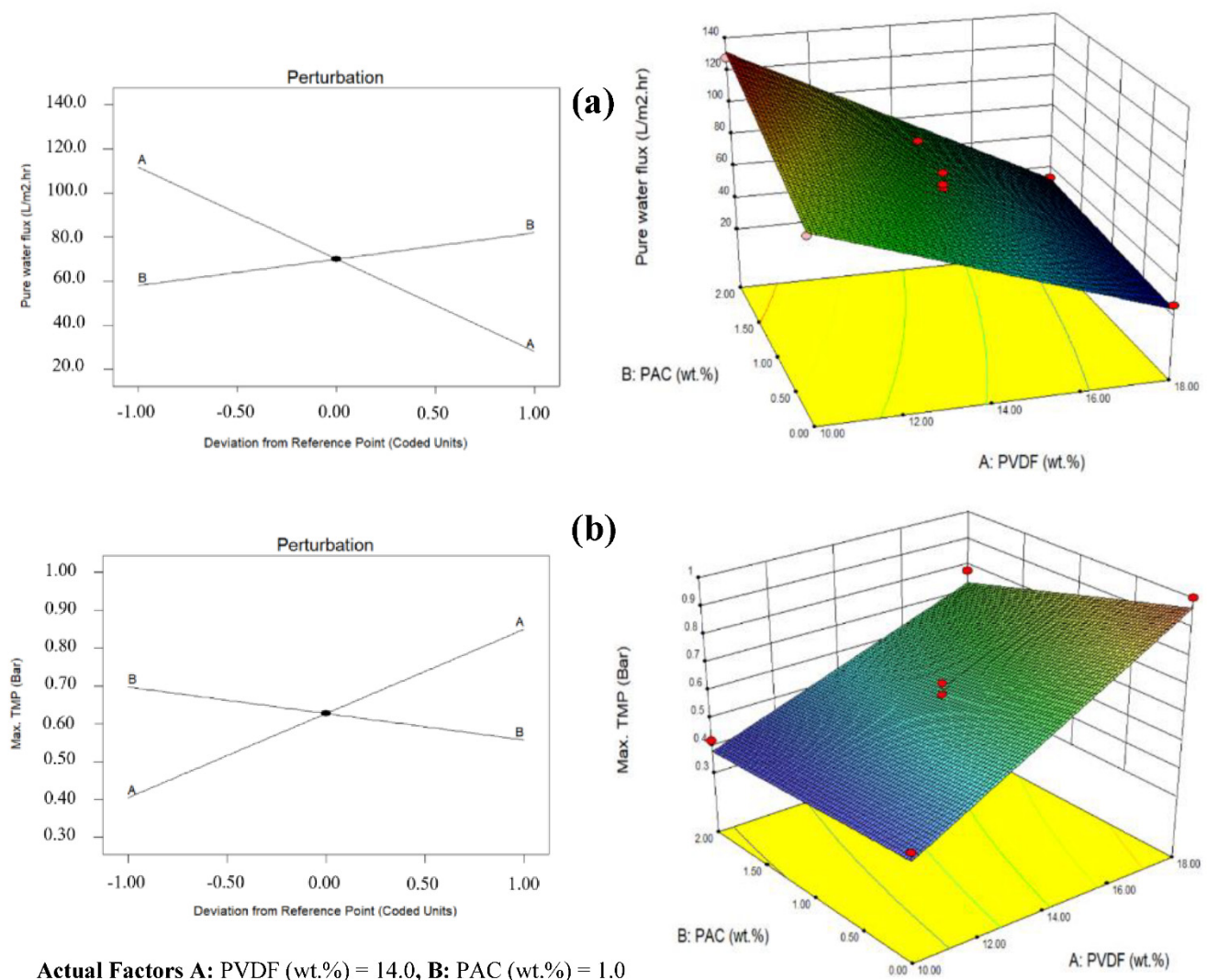
Figure 7. Perturbation plots (**left**) and 3D response surface (**right**) of PVDF-PAC fabricated membrane for (**a**) pure water flux and (**b**) max. TMP.

Minimum and maximum predicted pure fluxes (26.0 and 128.5 L/m^2·h) were found at the membrane compositions of 18.0 wt.% PVDF with 0.0 wt.% PAC, and 10.0 wt.% PVDF with 2.0 wt.% PAC, respectively. On the other hand, lowest and highest max. TMP according to the suggested model were found to be 0.38 and 0.98 bar at membranes of compositions (10.0 wt.%) PVDF with (2.0 wt.%) PAC, and 18.0 wt.% PVDF with 0.0 wt.% PAC, respectively. From the findings, membranes with lower PVDF concentration and high PAC concentration (10.0 wt.% PVDF and 2.0 wt.% PAC) exhibited the best water permeation and antifouling properties. Nonetheless, this membrane still falls short to produce the highest removing rates of COD, colour, and NH$_3$-N based on the previous discussion.

3.4. Fabricated Membrane Characterization

The morphology of produced membrane can explain the effect of dope composition on membrane performance. A collection of membranes composed from different concentrations of PVDF and PAC (wt.%) were chosen from the fabricated membranes to represent the different membrane compositions, and consequently to be investigated by the morphological studies. These membranes were: FM1 with the content of (10.0 wt.% PVDF-0.0 wt.% PAC) to represent minimum PVDF concentration with no PAC; (10.0 wt.% PVDF-2.0 wt.% PAC) to represent minimum PVDF with high PAC, denoted as FM2; (14.0 wt.% PVDF-1.0 wt.% PAC) to represent intermediate composition of both PVDF and

PAC, named FM3; and finally FM4 with 18.0 wt.% PVDF and 0.0 wt.% PAC to represent maximum concentration of PVDF without PAC.

The FTIR spectrum of PVDF-PAC fabricated membranes with the various compositions is illustrated in Figure 8. It is clearly observed from Figure 8 that membranes displayed semi-typical distinctive spectra along the range of 4000 and 400 cm^{-1}. Characteristic chemical groups are witnessed in the band of all membranes at waves with lengths 3020, 2990, 2370, 1400, 1070, 875, 590, and 490 cm^{-1} with altered vibrations of strength depends on the different membrane compositions. The spectrum shows bands at 2990 and 3020 cm^{-1} which are attributed to the symmetric and asymmetric stretching vibrations of C-H coming from ketones and carboxylic acids [54], where vibrations at 1070 and 1400 cm^{-1} presented the deformation peaks of C-F related to PVDF.
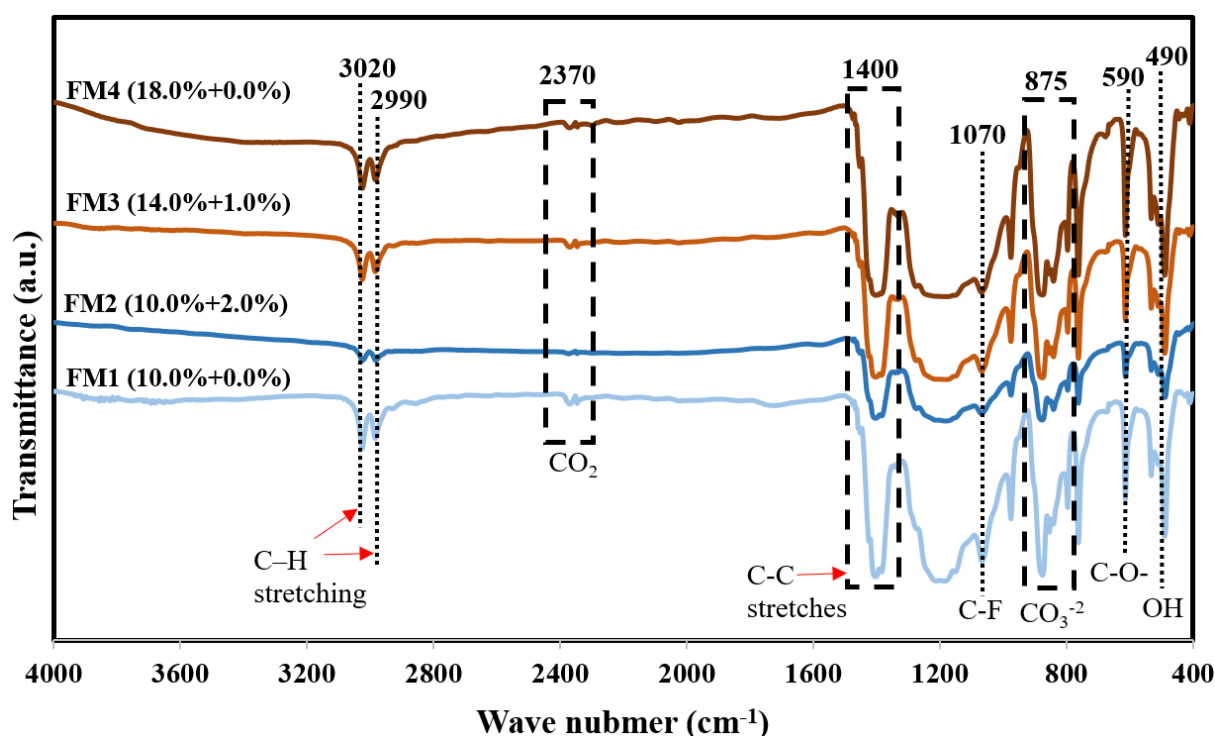

Figure 8. FTIR spectra for PVDF-PAC membranes with different concentrations.

The notable peaks of the various membranes at 2370, 875, and 590 cm^{-1}, assigned to CO_2, CO_3^{-2}, and C-O- groups, respectively, were the features distinctive of neutralization methanol, used after membrane casting [55]. Moreover, the OH group detected at 490 cm^{-1} is attributed to the DW used for membrane solidification during the casting process [56]. Figure 8 also confirmed that the recorded wave numbers in the spectrum of both membranes without PAC (FM1 and FM4) have higher frequencies in comparison with the spectrums of the other two membranes with PAC content (FM2 and FM3).

Furthermore, it could be observed that the peaks of the membrane with higher content of PAC (FM2) have lower vibrations compared with the membranes with lower PAC content (FM3). Evidently, the peaks become narrow with less strength at the increasing of PAC weight, indicating that the hydrogen bonds were constructed well between PVDF polymer chains and the hydroxyl groups from PAC, which reduces the PVDF hydrophobic tendency [57]. These outcomes confirmed that PAC was well integrated to PVDF membranes, and partially relocated on the membrane surface, which leads to membrane treatment efficiency enhancement.

To investigate the elemental composition present in the fabricated PVDF-PAC membranes with different compositions, EDX analysis was recorded in the binding energy region from 0 to 15 keV as exhibited in Figure 9. The PVDF characterized elements C

and F were clearly observed in the spectra of the pure PVDF membranes (without PAC), while the AL element, which characterizes the presence of PAC, appeared only at the PVDF membranes incorporated with PAC [33]. Figure 9b,d shows the EDX analysis of 2.0 and 1.0 wt.% PAC, respectively. It is clearly witnessed that the presence of PAC was presented well.
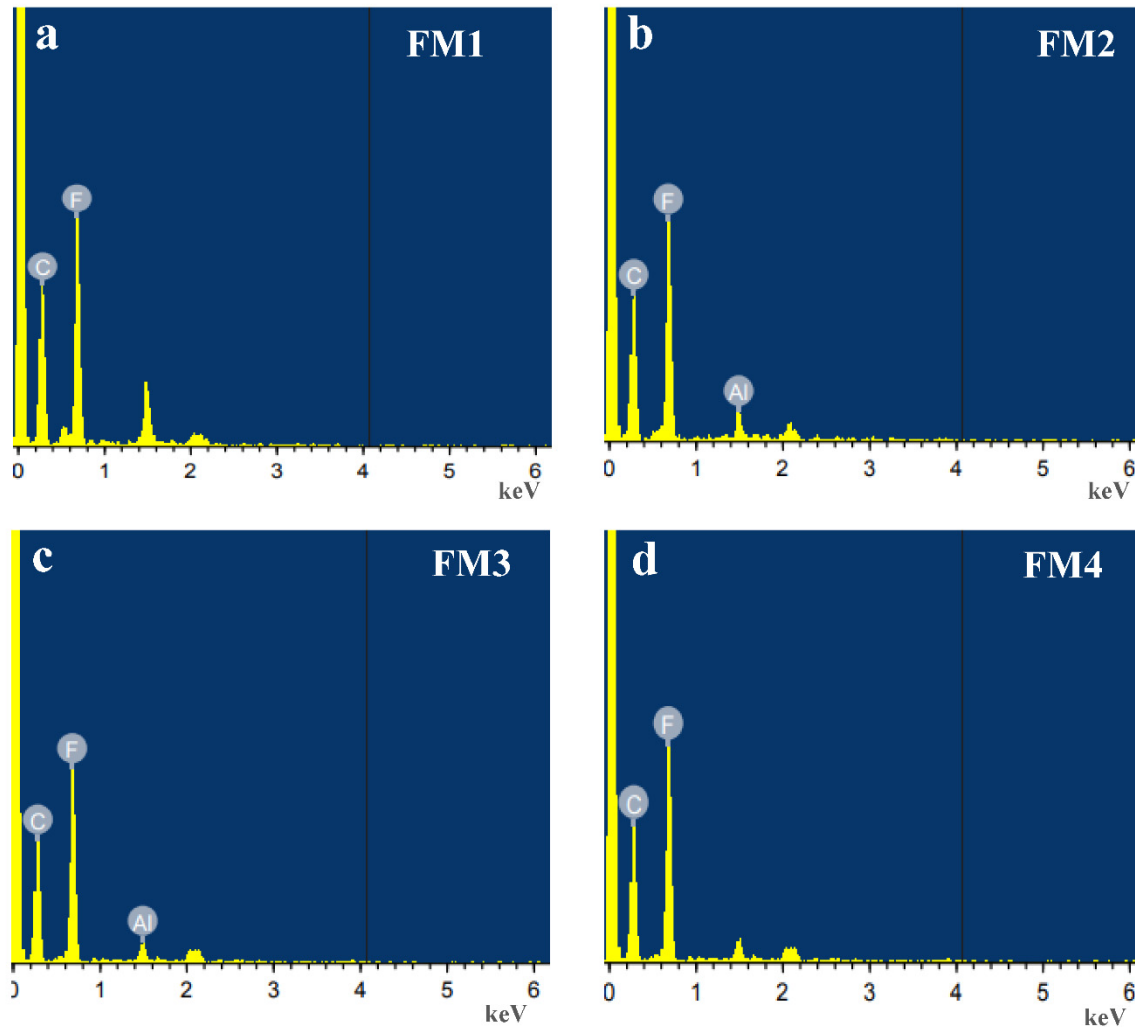

Figure 9. EDX analysis for the selected PVDF-PAC fabricated membranes with different compositions: (**a–d**) for (FM1–FM4).

Table 5 shows the atomic percentages of the different elemental compositions of the selected membranes (FM1–FM4). From the EDX findings, the weight percentages of elemental AL on the FM2 and FM3 were determined as 1.04 and 0.79, respectively, which confirmed the presence PAC with representative weights on the integrated membranes.

Table 5. Elemental compositions of selected PVDF-PAC fabricated membranes based on EDX mapping.

Sample	Composition (wt.%)		Elements Weight (%)			
	PVDF	**PAC**	**C**	**F**	**AL**	**Total**
FM1	10.0	0.0	61.69	38.31	0.00	100.00
FM2	10.0	2.0	60.85	38.11	1.04	100.00
FM3	14.0	1.0	61.04	38.17	0.79	100.00
FM4	18.0	0.0	60.63	39.37	0.00	100.00

Figure 10 presents the FESEM images for produced membranes with different compositions, which show the top surface morphology of membranes, along with its cross section. As can be seen from Figure 9a–d, there were many small pores available on the surface of FM1 membrane which contains the lowest PVDF polymer content (10.0 wt.%). Furthermore, the number and size of these pores start to be decreased, first on membrane FM3, with PVDF content 14.0 wt.% and PAC content 1.0 wt.%, followed by FM2 membrane with the highest PAC content (2.0 wt.%), while the membrane FM4 has a semi-impermeable surface due to its high PVDF polymer content (18.0 wt.%) with no PAC content. This was in agreement with the findings earlier discovered by Kunst and Sourirajan [58].
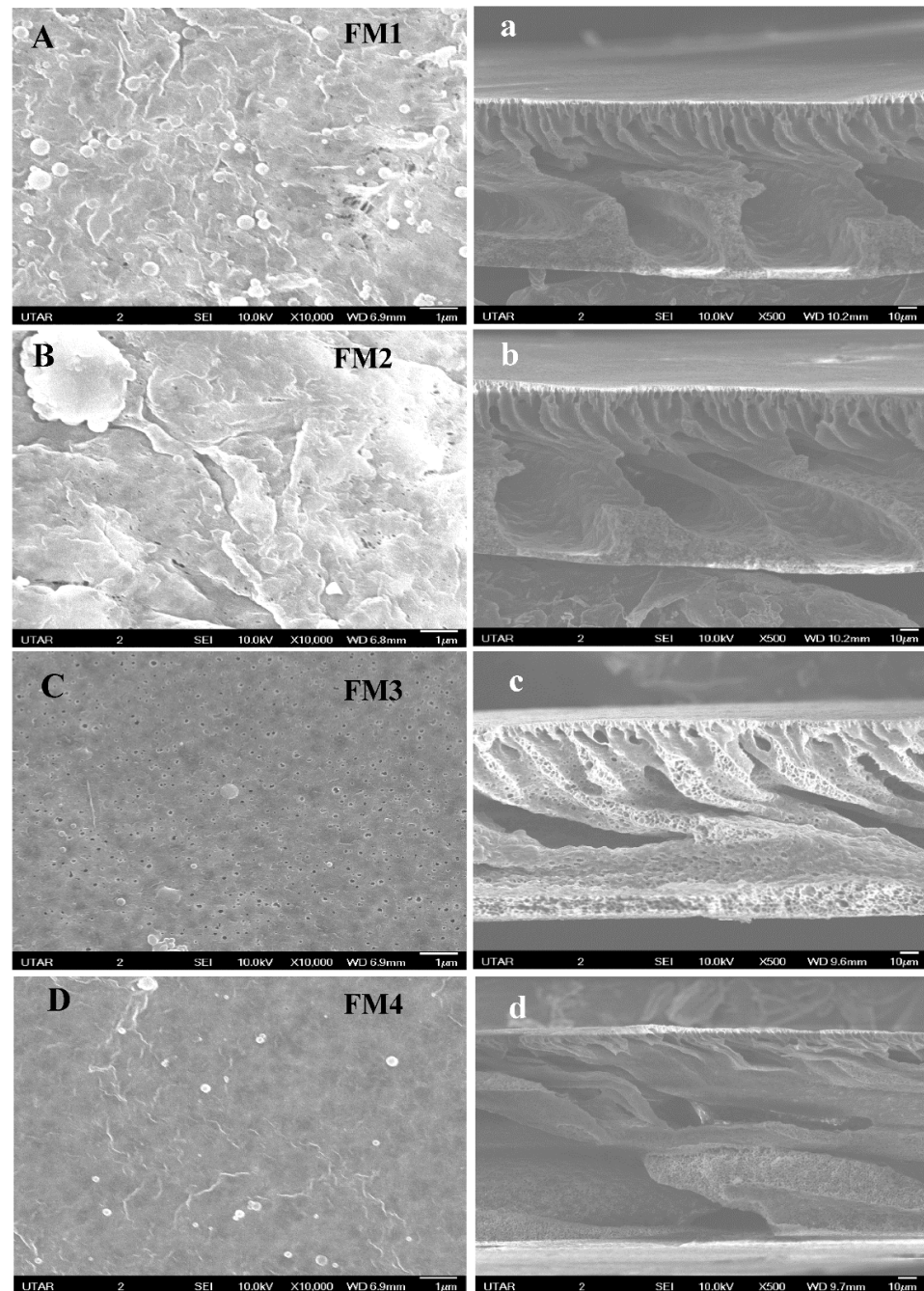

Figure 10. FESEM morphologies of PVDF-PAC membranes with different compositions (FM1 to FM4): (**a–d**) cross-sections and (**A–D**) top surfaces.

Referring to membrane cross sections on Figure 10a–d, all membranes display the formation of macrovoid with loosely packed structures. Typically, the membrane consists of two layers, which are a spongy porous support layer and a dense top finger-like layer. The establishment of these configurations can be attributed to the instantaneous demixing of polymer and solvent during the process of phase inversion.

FM1 membrane, with only PVDF and the weight of 10.0 wt.%, displayed an unimproved finger-like formation and a sponge-like support layer containing large, unconnected pores, delimited by polymer walls (see Figure 10a). The finger-like voids turn become flat, bigger, and even strained to the bottommost of the fabricated membranes with an increase in PAC concentration (i.e., in FM2 and FM3), and the spherical voids of the sponge-like structures connect more closely with themselves (Figure 10b,c). However, the FM4 membrane, containing the highest concentration of PVDF, gives thin, smaller, and non-stretched figure-like pores, with less connection to the little sponge-like pores located on the cross-section's bottom. This produces low membrane flux due to the greater amount of polymer contributing a higher membrane viscosity, which lead to a decease in the membrane porosity and pore size. The overall FESEM micrographs have proved the significant effect of the PAC presence in improving the fabricated membrane characteristic in terms of membrane rejection, and therefore removal rate of contaminants.

Furthermore, an AFM test was carried out to investigate the membrane top surface, along with its roughness, as shown in Figure 11. The FM2 membrane might contain some extra PAC particles which made its top surface rougher compared to others (Figure 11b). Having less depth of facial peaks and valleys, the FM4 membrane surface (Figure 11d) is relatively smooth due to containing only PVDF polymer which received a homogeneous mixing at the preparation phase of dope solution [59]. However, the peaks and valleys of FM1 and FM3 membranes reduced gradually compared to FM2, where FM3 has the smoothest surface compared with other membranes (see Figure 11a–d). To confirm all above observations, the values of membrane surface roughness (R_q and R_a) given in Figure 11 can be considered.
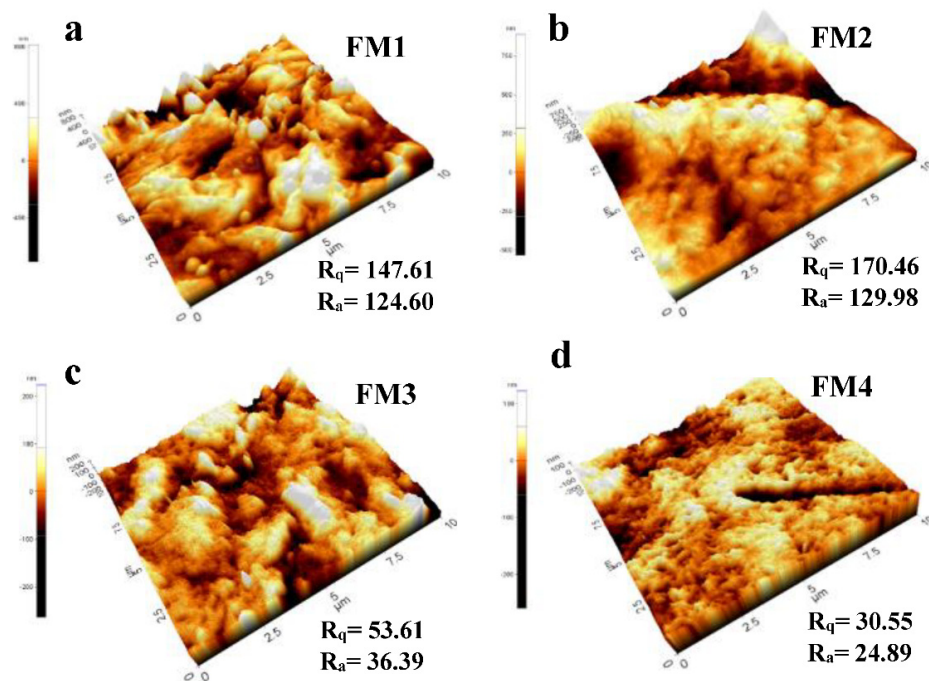
Figure 11. AFM top surface images with average membrane roughness values (nm) for different compositions of selected PVDF-PAC membranes: (**a–d**) for (FM1 to FM4).

For membrane permeability analysis, the impact of PAC addition to membrane permeability, in terms of porosity and average pore size, were evaluated for the produced PVDF membranes. As presented in Table 6, the porosity and average pore size of the fabricated PVDF membranes incorporated with PAC were higher than the other membranes without PAC. Based on Table 6, the resulted fabricated membranes were "micro-filtration", and the highest mean values of porosity and average pore size were achieved by FM2 membrane at the values 77.48% and 24.43 μm, respectively. On the other hand, the lowest values of the same corresponding permeability parameters were found using membrane FM4 at 48.38% and 12.15 μm, respectively. These findings agreed with the above morphological results.

Table 6. Permeability measurements for selected fabricated PVDF-PAC membranes.

Membrane	Composition		Porosity	Average Pore Size
	PVDF	**PAC**	**(%)** [a]	**(μm)** [a]
FM1	10.0	0.0	57.25 ± 0.18	15.34 ± 0.05
FM2	10.0	2.0	77.48 ± 0.50	24.43 ± 0.15
FM3	14.0	1.0	72.86 ± 0.20	21.27 ± 0.07
FM4	18.0	0.0	48.38 ± 0.62	12.15 ± 0.24

[a] Each parameter is expressed as average value ± standard deviation.

3.5. Membrane Treatment Optimization

The best synthesized membrane has been selected using the RSM tool, where the membrane efficiencies of COD, colour, and NH_3-N removal were optimized during this study.

Based on the DoE software, the operational conditions (PVDF weight and PAC weight) were targeted to be within the range. While the dependents of treatment performance (COD, colour, and NH_3-N removal) were chosen as ''maximum'' to achieve the ultimate filtration treatment. The other responses were remained "within the range". Accordingly, the optimization tool assimilates the singular desirability into a particular number, and then aims to optimize the function.

Consequently, the composition of the optimum membrane, together with respective rates of removal efficiency, were obtained. The optimum removals and their corresponding water flux and max. TMP are presented in Table 7.

Table 7. Predicted and experimental removal efficiencies of the optimum PVDF-PAC membrane with the corresponding operating condition.

Operating Conditions		Desirability	Optimum Conditions	
PVDF (wt.%)	**PAC (wt.%)**			
14.90	1.00	0.870	Selected	
Response		**Predicted Result**	**Experimental Result**	**Error (%)**
Removal of COD (%) *		35.34	36.63	3.65
Removal of colour (%) *		48.71	49.50	1.62
Removal of NH_3-N (%) *		22.00	23.84	8.36
Pure water flux (L/m²·h)		61.00	61.10	0.16
Max. TMP (bar)		0.67	0.64	4.48

* Optimum value.

The membrane with 14.9 wt.% of PVDF and 1.0 wt.% of PAC was found to be the optimum, and thus selected as the best membrane design, having optimum removal efficiency according to its highest desirability (0.870) [60].

As shown in Table 7, 35.34, 48.71, and 22.00% removal of COD, colour and NH_3-N, respectively, was predicted by the software under optimized operational conditions. The corresponding (non-optimized) water flux and max. TMP were found at the val-

ues 61.00 L/m^2·h and 0.67 bar, respectively. An additional experimentation was then performed to confirm the optimum findings.

As illustrated in Table 7, the error column indicates the differences between the predicted and laboratory values, which shows that the lab experiments agree well with the response values estimated by the software. However, less agreement between the predicted and the laboratory result was obtained in case of NH$_3$-N removal (8.36% error).

3.6. Membrane Performance Comparison with Other Reported Studies

The performance of the optimum fabricated membrane with other reported PVDF produced membranes is shown in Table 8. It can be noticed from Table 8 that the current study offered the smoother surface among the existing works based on the average roughness (R$_a$ = 36.39 nm), which accordingly improves the removing performance and antifouling properties of the created membrane [61]. There exists few values of pure flux that are higher than the achieved in the current work, such as the flux of 143.24 L/m^2·h produced by Penboon et al. [62]. The low value of pure water flux of the current work (61.00 L/m^2·h) could be ascribed to the differences in the experimental characteristics such as the type of wastewater or the rates of feed flow. In addition, the rejection efficiency in the current work is lower than previously reported, which could be solved through further enhancement of the produced membranes using hydrophilic additives such as PVA or PVP [25,57]. Based on previous studies, after saturation, membrane corroborated PAC can be washed back and reused [13,63].

Table 8. Comparison of performance with other modified PVDF membranes in wastewater treatment process.

Modification Agent	Pure Water Flux (L/m^2·h)	Feed Type & Feeding Rate (L/min)	Removal Rate Avg. (%)	Roughness (nm)	Reference
Titanium dioxide (TiO$_2$)	143.24	Wastewater FR = 0.850	86.1	-	[62]
Granular activated carbon (GAC)	13.90	Berlin tap water (Gravity driven)	88.0	-	[64]
Silica nanoparticles (SiO$_2$)	-	Cooking wastewater FR = 48.96	66.7	R$_a$ = 174	[65]
Reduced graphene oxide (rGO)	-	NaCl solution FR = 0.385	58.0	R$_a$ = 84	[66]
Powdered activated carbon (PAC)	61.00	SLF leachate FR = 0.20	35.35	R$_a$ = 36.39	Present study

4. Conclusions

The adsorbent material PAC was used to fabricate a novel PVDF membrane for the treatment of stabilized landfill leachate. The fabricated PVDF flat sheet membranes integrated with PAC showed better performance when compared with PVDF membrane (without PAC). The addition of PAC effectively enhanced the removal rate and the fouling control parameters of produced membranes. Increasing PAC content to a certain value has a positive influence on the removal efficiency of COD, colour, and NH$_3$-N, as well as on membrane characteristics. Operational optimization was performed using RSM to select the optimum membrane design in terms of the removal efficiency. The best membrane composition was found at (14.9 wt.%) PVDF and (1.0 wt.%) PAC, which removed 36.63% of COD, 49.50% of colour, and 23.84% of NH$_3$-N. This was in agreement with the predicted removals. The corresponding experimental values of water flux and max. TMP also agreed with the prediction, with the values of 61.10 L/m^2·h and 0.64 bar, respectively. The performance and structure of fabricated membranes were investigated by filtration tests, FTIR, FESEM, and AFM spectroscopy. In general, this work shows the potential of treatment and hydrophilic improvement of hydrophobic PVDF polymer membranes using

PAC. For further removal efficiency, membrane properties or practice could be improved by either adding a hydrophilic material, or applying pre-treatment process such as adsorption via PAC.

References

1. Xu, Y.; Chen, C.; Li, X.; Lin, J.; Liao, Y.; Jin, Z. Recovery of humic substances from leachate nanofiltration concentrate by a two-stage process of tight ultrafiltration membrane. *J. Clean. Prod.* **2017**, *161*, 84–94. [CrossRef]
2. Bashir, M.J.K.; Jun, Y.Z.; Yi, L.J.; Abushammala, M.F.M.; Amr, S.S.A.; Pratt, L.M. Appraisal of student's awareness and practices on waste management and recycling in the Malaysian University's student hostel area. *J. Mater. Cycles Waste Manag.* **2020**, *22*, 916–927. [CrossRef]
3. Abuabdou, S.M.A.; Ahmad, W.; Aun, N.C.; Bashir, M.J.K. A review of anaerobic membrane bioreactors (AnMBR) for the treatment of highly contaminated landfill leachate and biogas production: Effectiveness, limitations and future perspectives. *J. Clean. Prod.* **2020**, *255*, 120215. [CrossRef]
4. Azmi, N.B.; Bashir, M.J.K.; Sethupathi, S.; Ng, C.A. Anaerobic stabilized landfill leachate treatment using chemically activated sugarcane bagasse activated carbon: Kinetic and equilibrium study. *Desalin. Water Treat.* **2016**, *57*, 3916–3927. [CrossRef]
5. Abuabdou, S.M.A.; Teng, O.W.; Bashir, M.J.K.; Aun, N.C.; Sethupathi, S.; Pratt, L.M. Treatment of tropical stabilised landfill leachate using palm oil fuel ashisothermal and kinetic studies. *Desalin. Water Treat.* **2019**, *144*, 201–210. [CrossRef]
6. Banch, T.J.H.; Hanafiah, M.M.; Alkarkhi, A.F.M.; Abu Amr, S.S. Factorial Design and Optimization of Landfill Leachate Treatment Using Tannin-Based Natural Coagulant. *Polymers* **2019**, *11*, 1349. [CrossRef]
7. Xu, Q.; Siracusa, G.; Di Gregorio, S.; Yuan, Q. COD removal from biologically stabilized landfill leachate using Advanced Oxidation Processes (AOPs). *Process. Saf. Environ. Prot.* **2018**, *120*, 278–285. [CrossRef]
8. Guvenc, S.Y.; Dincer, K.; Varank, G. Performance of electrocoagulation and electro-Fenton processes for treatment of nano filtration concentrate of biologically stabilized landfill leachate. *J. Water Process Eng.* **2019**, *31*, 100863–100875. [CrossRef]
9. Abu Amr, S.S.; Zakaria, S.N.F.; Aziz, H.A. Performance of combined ozone and zirconium tetrachloride in stabilized landfill leachate treatment. *J. Mater. Cycles Waste Manag.* **2016**, *19*, 1384–1390. [CrossRef]
10. Zielinska, M.; Kulikowska, D.; Stanczak, M. Adsorption—Membrane process for treatment of stabilized municipal landfill leachate. *Waste Manag.* **2020**, *114*, 174–182. [CrossRef]
11. Abuabdou, S.M.A.; Bashir, M.J.K.; Aun, N.C.; Sethupathi, S. Applicability of anaerobic membrane bioreactors for landfill leachate treatment: Review and opportunity. *IOP Conf. Ser. Earth Environ. Sci.* **2018**, *140*, 012033–012042. [CrossRef]
12. Shen, J.; Zhang, Q.; Yin, Q.; Cui, Z.; Li, W.; Xing, W. Fabrication and characterization of amphiphilic PVDF copolymer ultra filtration membrane with high anti-fouling property. *J. Memb. Sci.* **2017**, *521*, 95–103. [CrossRef]
13. Ng, C.A.; Wong, L.Y.; Bashir, M.J.K.; Ng, S.L. Development of Hybrid Polymeric Polyerthersulfone (PES) Membrane Incorporated with Powdered Activated Carbon (PAC) for Palm Oil Mill Effluent (POME) Treatment. *Int. J. Integr. Eng. Spec. Issue Civ. Environ. Eng.* **2018**, *10*, 137–141. [CrossRef]
14. Krzeminski, P.; Leverette, L.; Malamis, S.; Katsou, E. Membrane bioreactors—A review on recent developments in energy reduction, fouling control, novel configurations, LCA and market prospects. *J. Memb. Sci.* **2017**, *527*, 207–227. [CrossRef]
15. Shehzad, A.; Bashir, M.J.K.; Sethupathi, S.; Lim, J. Simultaneous Removal of Organic and Inorganic Pollutants From Landfill Leachate Using Sea Mango Derived Activated Carbon via Microwave Induced Activation. *Int. J. Chem. React. Eng.* **2016**, *14*, 991–1001. [CrossRef]
16. Miller, D.J.; Paul, D.R.; Freeman, B.D. An improved method for surface modification of porous water purification membranes. *Polymer* **2014**, *55*, 1375–1383. [CrossRef]
17. Jankhah, S.; Bérubé, P.R. Pulse bubble sparging for fouling control. *Sep. Purif. Technol.* **2014**, *134*, 58–65. [CrossRef]

18. Venkataganesh, B.; Maiti, A.; Bhattacharjee, S.; De, S. Electric field assisted cross flow micellar enhanced ultrafiltration for removal of naphthenic acid. *Sep. Purif. Technol.* **2012**, *98*, 36–45. [CrossRef]

19. Crittenden, J.C.; Trussell, R.R.; Hand, D.W.; Howe, K.J.; Tchobanoglous, G. *MWH's Water Treatment: Principles and Design*; John Wiley & Sons: Hoboken, NJ, USA, 2012.

20. Ismail, N.H.; Salleh, W.N.W.; Ismail, A.F.; Hasbullah, H.; Yusof, N.; Aziz, F.; Jaafar, J. Hydrophilic polymer-based membrane for oily wastewater treatment: A review. *Sep. Purif. Technol.* **2020**, *233*, 116007. [CrossRef]

21. Nawi, N.I.M.; Bilad, M.R.; Nordin, N.A.H.M.; Mavukkandy, M.O.; Putra, Z.A.; Wirzal, M.D.H.; Jaafar, J.; Khan, A.L. Exploiting the interplay between liquid-liquid demixing and crystallization of the PVDF membrane for membrane distillation. *Int. J. Polym. Sci.* **2018**, *2018*, 1–10. [CrossRef]

22. Ji, J.; Liu, F.; Hashim, N.A.; Abed, M.R.M.; Li, K. Reactive & Functional Polymers Poly (vinylidene fluoride) (PVDF) membranes for fluid separation. *React. Funct. Polym.* **2015**, *86*, 134–153. [CrossRef]

23. Bashir, M.J.K.; Xian, T.M.; Shehzad, A.; Sethupahi, S.; Aun, N.C.; Amr, S.A. Sequential treatment for landfill leachate by applying coagulation-adsorption process. *Geosystem Eng.* **2017**, *20*, 9–20. [CrossRef]

24. Lv, J.; Zhang, G.; Zhang, H.; Zhao, C.; Yang, F. Improvement of antifouling performances for modified PVDF ultrafiltration membrane with hydrophilic cellulose nanocrystal. *Appl. Surf. Sci.* **2018**, *440*, 1091–1100. [CrossRef]

25. Mokhtar, N.M.; Lau, W.J.; Ng, B.C.; Ismail, A.F.; Veerasamy, D. Preparation and characterization of PVDF membranes incorporated with different additives for dyeing solution treatment using membrane distillation. *Desalin. Water Treat.* **2015**, *56*, 1999–2012. [CrossRef]

26. Zhou, A.; Jia, R.; Wang, Y.; Sun, S.; Xin, X.; Wang, M.; Zhao, Q.; Zhu, H. Abatement of sulfadiazine in water under a modified ultrafiltration membrane (PVDF-PVP-TiO$_2$-dopamine) filtration-photocatalysis system. *Sep. Purif. Technol.* **2020**, *234*. [CrossRef]

27. Jhaveri, J.H.; Murthy, Z.V.P. A comprehensive review on anti-fouling nanocomposite membranes for pressure driven membrane separation processes. *Desalination* **2016**, *379*, 137–154. [CrossRef]

28. Zhang, J.; Wang, Q.; Wang, Z.; Zhu, C.; Wu, Z. Modification of poly (vinylidene fluoride)/polyethersulfone blend membrane with polyvinyl alcohol for improving antifouling ability. *J. Memb. Sci.* **2014**, *466*, 293–301. [CrossRef]

29. Wong, L.Y.; Ng, C.A.; Bashir, M.J.K.; Cheah, C.K.; Leong, K. Desalination and Water Treatment Membrane bioreactor performance improvement by adding adsorbent and coagulant: A comparative study. *Desalin. Water Treat.* **2015**, 37–41. [CrossRef]

30. Wong, S.; Ngadi, N.; Inuwa, I.M.; Hassan, O. Recent advances in applications of activated carbon from biowaste for wastewater treatment: A short review. *J. Clean. Prod.* **2018**, *175*, 361–375. [CrossRef]

31. Bashir, M.J.K.; Wong, J.W.; Sethupathi, S.; Aun, N.C.; Wei, L.J. Preparation of Palm Oil Mill Effluent Sludge Biochar for the Treatment of Landfill Leachate. *MATEC Web Conf.* **2017**, *103*, 1–8. [CrossRef]

32. APHA Water Environment Federation. *Standard Methods for the Examination of Water and Wastewater*, 22nd ed.; APHA: Washington, DC, USA, 2012.

33. Abuabdou, S.M.A.; Bashir, M.J.K.; Aun, N.C.; Sethupathi, S.; Yong, W.L. Development of a novel polyvinylidene fluoride membrane integrated with palm oil fuel ash for stabilized landfill leachate treatment. *J. Clean. Prod.* **2021**, *311*, 127677. [CrossRef]

34. Mertens, M.; Van Dyck, T.; Van Goethem, C.; Gebreyohannes, A.Y.; Vankelecom, I.F.J. Development of a polyvinylidene di fluoride membrane for nano filtration. *J. Memb. Sci.* **2018**, *557*, 24–29. [CrossRef]

35. Tan, S.T.; Ho, W.S.; Hashim, H.; Lee, C.T.; Taib, M.R.; Ho, C.S. Energy, economic and environmental (3E) analysis of waste-to-energy (WTE) strategies for municipal solid waste (MSW) management in Malaysia. *Energy Convers. Manag.* **2015**, *102*, 111–120. [CrossRef]

36. Abu Amr, S.S.; Aziz, H.A.; Bashir, M.J.K. Application of response surface methodology (RSM) for optimization of semi-aerobic landfill leachate treatment using ozone. *Appl. Water Sci.* **2014**, *4*, 231–239. [CrossRef]

37. Stat-Ease Inc. Multifactor RSM Tutorial. Available online: https://www.statease.com/ (accessed on 30 July 2021).

38. Naragintia, S.; Yua, Y.-Y.; Fanga, Z.; Yong, Y.-C. Novel tetrahedral Ag$_3$PO$_4$@N-rGO for photocatalytic detoxification of sulfamethoxazole: Process optimization, transformation pathways and biotoxicity assessment. *Chem. Eng. J.* **2019**, *375*, 122035. [CrossRef]

39. Ghani, Z.A.; Suffian, M.; Qamaruz, N.; Faiz, M.; Ahmad, M. Optimization of preparation conditions for activated carbon from banana pseudo-stem using response surface methodology on removal of color and COD from landfill leachate. *Waste Manag.* **2017**, *62*, 177–187. [CrossRef]

40. Ike, I.A.; Dumée, L.F.; Groth, A.; Orbell, J.D.; Duke, M. Effects of dope sonication and hydrophilic polymer addition on the properties of low pressure PVDF mixed matrix membranes. *J. Memb. Sci.* **2017**, *540*, 200–211. [CrossRef]

41. Nejati, S.; Boo, C.; Osuji, C.O.; Elimelech, M. Engineering flat sheet microporous PVDF films for membrane distillation. *J. Memb. Sci.* **2015**, *492*, 355–363. [CrossRef]

42. Fan, H.; Peng, Y. Application of PVDF membranes in desalination and comparison of the VMD and DCMD processes. *Chem. Eng. Sci.* **2012**, *79*, 94–102. [CrossRef]

43. Aziz, H.A.; Mojiri, A. *Wastewater Engineering: Advanced Wastewater Treatment Systems*, 1st ed.; IJSR Publications: Raipur, India, 2014; ISBN 2322-4657.

44. Chidambaram, T.; Oren, Y.; Noel, M. Fouling of nanofiltration membranes by dyes during brine recovery from textile dye bath wastewater. *Chem. Eng. J.* **2015**, *262*, 156–168. [CrossRef]

45. Zheng, Y.; Zhang, W.; Tang, B.; Ding, J.; Zheng, Y.; Zhang, Z. Membrane fouling mechanism of biofilm-membrane bioreactor (BF-MBR): Pore blocking model and membrane cleaning. *Bioresour. Technol.* **2018**, *250*, 398–405. [CrossRef]

46. Chen, X.; Zhao, B.; Zhao, L.; Bi, S.; Han, P.; Chen, L. Temperature- and pH-responsive properties of poly(vinylidene fluoride) membranes functionalized by blending microgels. *RSC Adv.* **2014**, *4*, 29933–29945. [CrossRef]

47. *Environmental Requirements: A Guide for Investors, Department of Environment*; Ministry of Natural Resources and Environment: Kuala Lumpur, Malaysia, 2010.

48. Kemal, A.; Siraj, K.; Michael, W.H. Adsorption of Cu (II) and Cd (II) onto Activated Carbon Prepared from Pumpkin Seed Shell. *J. Environ. Sci. Pollut. Res.* **2019**, *5*, 328–333. [CrossRef]

49. Aslam, M.; Ahmad, R.; Kim, J. Recent developments in biofouling control in membrane bioreactors for domestic wastewater treatment. *Sep. Purif. Technol.* **2018**, *206*, 297–315. [CrossRef]

50. Ali, I.; Bamaga, O.A.; Gzara, L.; Bassyouni, M. Assessment of Blend PVDF Membranes, and the Effect of Polymer Concentration and Blend Composition. *J. Membr.* **2018**, *8*, 13. [CrossRef] [PubMed]

51. Gunst, R.F.; Stein, R.; Hatcher, L.; Heckler, C.E.; Adams, B.M.; Kit, T.S.; Fink, A.; Lawson, J. *Response Surface Methodology: Process and Product Optimization Using Designed Experiments Book Reviews*; John Wiley & Sons: Hoboken, NJ, USA, 2012.

52. Abuabdou, S.M.A.; Teng, O.W.; Bashir, M.J.K.; Aun, N.C.; Sethupathi, S. Adsorptive treatment of stabilized landfill leachate using activated palm oil fuel ash (POFA). *AIP Conf. Proc.* **2019**, *2157*, 20002–20008. [CrossRef]

53. Khadijah, S.; Ha, M.; Othman, D.; Harun, Z.; Ismail, A.F.; Iwamoto, Y.; Honda, S.; Rahman, M.A.; Jaafar, J.; Gani, P.; et al. Effect of fabrication parameters on physical properties of metakaolin-based ceramic hollow fi bre membrane (CHFM). *Ceram. Int.* **2016**, *42*, 15547–15558. [CrossRef]

54. Fumoto, E.; Sato, S.; Takanohashi, T. Determination of Carbonyl Functional Groups in Heavy Oil Using Infrared Spectroscopy. *Energy Fuels* **2020**, *34*, 5231–5235. [CrossRef]

55. Gurkan, B.E.; de la Fuente, J.C.; Mindrup, E.M.; Ficke, L.E.; Goodrich, B.F.; Price, E.A.; Schneider, W.F.; Brennecke, A.J.F. Equimolar CO_2 Absorption by Anion-Functionalized Ionic Liquids. *J. Am. Chem. Soc.* **2010**, *132*, 2116–2117. [CrossRef] [PubMed]

56. Guo, D.; Xiao, Y.; Li, T.; Zhou, Q.; Shen, L.; Li, R.; Xu, Y.; Lin, H. Fabrication of high-performance composite nanofiltration membranes for dye wastewater treatment: Mussel-inspired layer-by-layer self-assembly. *J. Colloid Interface Sci.* **2020**, *560*, 273–283. [CrossRef]

57. Zhang, J.; Wang, Z.; Wang, Q.; Ma, J.; Cao, J.; Hu, W.; Wu, Z. Relationship between polymers compatibility and casting solution stability in fabricating PVDF/PVA membranes. *J. Memb. Sci.* **2017**, *537*, 263–271. [CrossRef]

58. Kunst, B.; Sourirajan, S. An approach to the development of cellulose acetate ultrafiltration membranes. *J. Appl. Polym. Sci.* **1974**, *18*, 3423–3434. [CrossRef]

59. Tae, J.; Kim, J.F.; Hyun, H.; Drioli, E.; Moo, Y. Understanding the non-solvent induced phase separation (NIPS) effect during the fabrication of microporous PVDF membranes via thermally induced phase separation (TIPS). *J. Memb. Sci.* **2016**, *514*, 250–263. [CrossRef]

60. Bezerra, M.A.; Santelli, R.E.; Oliveira, E.P.; Villar, L.S.; Escaleira, L.A. Response surface methodology (RSM) as a tool for optimization in analytical chemistry. *Talanta* **2008**, *76*, 965–977. [CrossRef]

61. Ayyaru, S.; Ahn, Y.H. Application of sulfonic acid group functionalized graphene oxide to improve hydrophilicity, permeability, and antifouling of PVDF nanocomposite ultrafiltration membranes. *J. Memb. Sci.* **2017**, *525*, 210–219. [CrossRef]

62. Penboon, L.; Khrueakham, A.; Sairiam, S. TiO_2 coated on PVDF membrane for dye wastewater treatment by a photocatalytic membrane. *Water Sci. Technol.* **2019**, *79*, 958–966. [CrossRef]

63. Tai, C.Y.; Abuabdou, S.M.A.; Ng, C.A.; Gan, C.H.; Bashir, M.J.K. Performance of hybrid anaerobic membrane bioreactors (AnMBRs) augmented with activated carbon in treating palm oil mill effluent (POME). *Desalin. Water Treat.* **2020**, *26156*, 1–8. [CrossRef]

64. Schumann, P.; Andrade, J.A.O.; Jekel, M.; Ruhl, A.S. Packing granular activated carbon into a submerged gravity-driven fl at sheet membrane module for decentralized water treatment. *J. Water Process Eng.* **2020**, *38*, 101517. [CrossRef]

65. Li, J.; Guo, S.; Xu, Z.; Li, J.; Pan, Z.; Du, Z.; Cheng, F. Preparation of omniphobic PVDF membranes with silica nanoparticles for treating coking wastewater using direct contact membrane distillation: Electrostatic adsorption vs. chemical bonding. *J. Memb. Sci.* **2019**, *574*, 349–357. [CrossRef]

66. Abdel-karim, A.; Luque-alled, J.M.; Leaper, S.; Alberto, M.; Fan, X.; Vijayaraghavan, A.; Gad-allah, T.A.; El-kalliny, A.S.; Szekely, G.; Ahmed, S.I.A.; et al. PVDF membranes containing reduced graphene oxide: Effect of degree of reduction on membrane distillation performance. *Desalination* **2019**, *452*, 196–207. [CrossRef]